

# Photophysical Properties of the Re<sup>I</sup> and Ru<sup>II</sup> Complexes of a New C<sub>60</sub>-Substituted Bipyridine Ligand

Nicola Armaroli,<sup>\*[a]</sup> Gianluca Accorsi,<sup>[a]</sup> Delphine Felder,<sup>[b]</sup> and Jean-François Nierengarten<sup>\*[b]</sup>

*Dedicated to Professor François Diederich on the occasion of his 50th birthday*

**Abstract:** The rhenium(I) and ruthenium(II) complexes of a fullerene-substituted bipyridine ligand have been prepared. Electrochemical studies indicate that some ground state electronic interaction between the fullerene subunit and the metal-complexed moiety are present in the Re<sup>I</sup> but not the Ru<sup>II</sup> complex. The photophysical properties have been investigated by steady-state and time-resolved UV/Vis-NIR luminescence spectroscopy and nanosecond laser flash photolysis in CH<sub>2</sub>Cl<sub>2</sub> solution, and compared to those of the corresponding model compounds. Excitation of the methanofullerene moiety in the dyads does not lead to excited state intercomponent interactions. Instead, excitation of the metal-complexed unit shows that the lowest triplet metal-to-

ligand-charge-transfer excited state (<sup>3</sup>MLCT) centered on the Re<sup>I</sup>- or Ru<sup>II</sup>-type unit is quenched with a rate constant of about  $2.5 \times 10^8 \text{ s}^{-1}$ . The quenching is attributed to an electron-transfer (EIT) process leading to the reduction of the carbon sphere, as determined by luminescence spectroscopy for the Ru<sup>II</sup> dyad. Experimental detection of electron transfer in the Re<sup>I</sup> dyad is prevented due to the unfavorable absorption of the metal-complexed moiety relative to the fullerene unit. However, it can be postulated on the basis of energetic/kinetic arguments and by comparison

**Keywords:** electron transfer • fullerene • rhenium • ruthenium • triplet sensitization

with the Ru<sup>II</sup>-type array. The primary EIT process is followed by charge-recombination to give the lowest-lying fullerene triplet excited state (<sup>3</sup>C<sub>60</sub>) with quantitative yield, as determined by sensitized singlet oxygen luminescence experiments. Direct <sup>3</sup>MLCT → <sup>3</sup>C<sub>60</sub> triplet-triplet energy-transfer (EnT) does not successfully compete with EIT since it is highly exoergonic and located in the Marcus inverted region. The quantum yield of singlet oxygen sensitization ( $\Phi_{\Delta}$ ) of the Re<sup>I</sup>-based dyad is found to be lower (0.80) than for the corresponding Ru<sup>II</sup> derivative (1.0). This is likely to be the consequence of different conformational structures for the two dyads, rather than a different yield of <sup>3</sup>C<sub>60</sub> formation.

## Introduction

The ability of fullerenes to act as electron acceptors make them attractive for participation in photoinduced electron-transfer (EIT) processes.<sup>[1–5]</sup> It is therefore not surprising that a large number of fullerene multicomponent architectures, including sophisticated tetrads,<sup>[6]</sup> hexads,<sup>[7]</sup> and dendrimers<sup>[8]</sup> have been prepared and their photophysical properties investigated in detail. One of the main goals of this research

activity is that of producing, by means of light inputs, long-lived and high-energy intramolecular charge-separated states, which can be exploited for practical applications such as solar energy conversion.<sup>[9–11]</sup>

The long lived metal-to-ligand-charge-transfer (MLCT) excited states characterizing some transition metal complexes such as tris(2,2'-bipyridine)ruthenium(II),<sup>[12]</sup> bis(1,10-phenanthroline)copper(I),<sup>[13]</sup> or (2,2'-bipyridine)rhenium(I)<sup>[14]</sup> have been widely exploited to design multicomponent molecular architectures featuring photoinduced electron- and energy-transfer (EnT) processes.<sup>[13, 15]</sup> Interestingly, the MLCT excited states of these compounds have a marked reducing character that, in principle, make them ideal partners for the construction of donor-acceptor systems with C<sub>60</sub> fullerenes. However, not many examples of such arrays have been reported to date, and they include only Ru<sup>II</sup><sup>[16–20]</sup> or Cu<sup>I</sup>,<sup>[8, 21]</sup> but not Re<sup>I</sup> complexes.

Herein, we report on the preparation of the first rhenium(I) complex of a methanofullerene-substituted bipyridine ligand

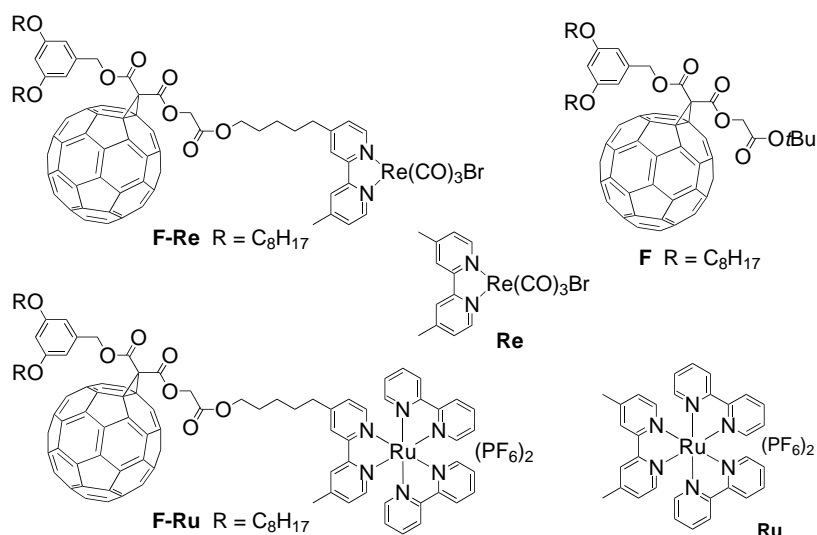
[a] Dr. N. Armaroli, Dr. G. Accorsi  
Istituto di Fotochimica e Radiazioni d'Alta Energia del CNR  
Via Gobetti 101, 40129 Bologna (Italy)  
Fax: (+39)051-6399844  
E-mail: armaroli@frae.bo.cnr.it

[b] Dr. J.-F. Nierengarten, Dr. D. Felder  
Groupe des Matériaux Organiques  
Institut de Physique et Chimie des Matériaux de Strasbourg  
Université Louis Pasteur et CNRS (UMR7504)  
23 rue du Loess, 67037 Strasbourg (France)  
E-mail: niereng@ipcms.u-strasbg.fr

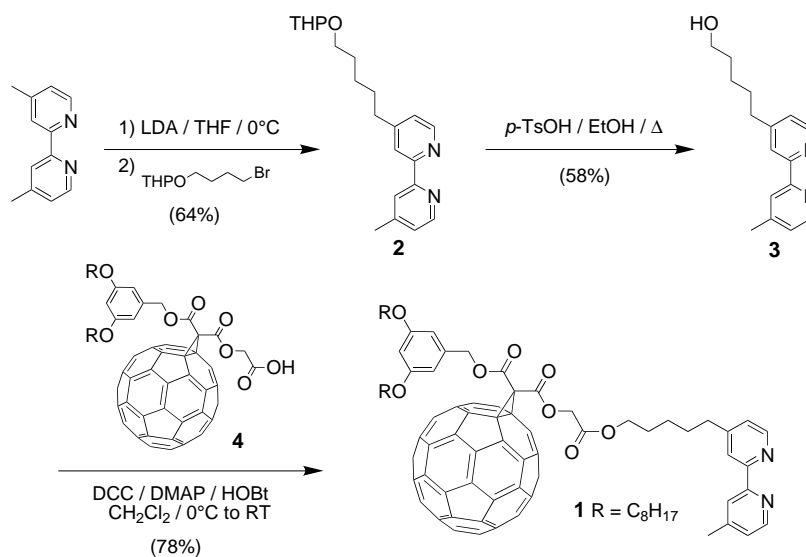
(**F-Re**) (Scheme 1), and of the corresponding  $[\text{Ru}(\text{bpy})_3]^{2+}$ -type dyad (**F-Ru**). The electrochemical properties of **F-Re** and **F-Ru** have been investigated and compared to those of the corresponding model compounds **F**,<sup>[22]</sup> **Re**, and **Ru**. By means of steady-state and time-resolved UV/Vis-NIR luminescence spectroscopy and nano-second laser-flash photolysis we showed that, in  $\text{CH}_2\text{Cl}_2$  solution, the lowest-lying triplet metal-to-ligand-charge-transfer excited state ( $^3\text{MLCT}$ ) centered on the  $\text{Ru}^{\text{II}}$ -type unit is quenched by EIT leading to the reduction of the carbon sphere, followed by charge-recombination to give the lowest fullerene triplet excited state ( $^3\text{C}_{60}$ ) with quantitative yield. The unfavorable absorption of the metal-complexed moiety relative to the fullerene unit prevents experimental detection of electron transfer in the  $\text{Re}^{\text{I}}$  dyad. However, such a quenching mechanism can be supported by energetic arguments and comparison with the  $\text{Ru}^{\text{II}}$ -type array. The charge-separation/charge-recombination sequence is present both at 298 and 77 K for **F-Re** but only at 298 K for **F-Ru**. Interestingly, the direct  $^3\text{MLCT} \rightarrow ^3\text{C}_{60}$  triplet-triplet EnT is found to be uncompetitive with EIT. Finally, the quantum yield of singlet oxygen sensitization ( $\Phi_{\Delta}$ ) is found to be different for the two dyads and this is ascribed to structural factors related to the flexibility of the interchromophoric spacer.

## Results and Discussion

**Synthesis:** The preparation of fullerene-substituted bipyridine ligand **1** is depicted in Scheme 2. Compound **2** was obtained from 4,4'-dimethyl-2,2'-bipyridine by deprotonation of one of the methyl groups with lithium diisopropylamide (LDA) to generate the corresponding carbanionic species, followed by reaction with 4-bromobutyl tetrahydropyran-2-yl ether.<sup>[23]</sup> Subsequent cleavage of the 3,4,5,6-tetrahydro-2*H*-pyranil (THP) protecting group, followed by treatment of the resulting **3** with **4**<sup>[22]</sup> under esterification conditions (*N,N'*-dicyclohexylcarbodiimide (DCC), 4-dimethylaminopyridine (DMAP), 1-hydroxybenzotriazole (HOBt)) yielded ligand **1**.



Scheme 1. Structures of compounds **F-Re**, **F-Ru**, **Re**, **Ru**, and **F**.



Scheme 2. Preparation of Ligand **1**.

The corresponding rhenium(I) complex **F-Re** was then obtained by reaction of **1** with  $[\text{Re}(\text{CO})_5\text{Br}]$  in refluxing toluene. Model compound **Re** was prepared under similar conditions from the commercially available 4,4'-dimethyl-2,2'-bipyridine and  $[\text{Re}(\text{CO})_5\text{Br}]$ . **F-Ru** and **Ru** were prepared by reacting the corresponding ligand with  $[\text{Ru}(\text{bpy})_2\text{Cl}_2]$  under standard conditions.<sup>[18]</sup> All of the spectroscopic and elemental analysis data were consistent with the proposed molecular structures.

**Electrochemistry:** The electrochemical properties of **F-Re**, **F-Ru**, **F**, **Ru**, and **Re** were investigated by cyclic voltammetry (CV) in  $\text{CH}_2\text{Cl}_2 + 0.1\text{M } n\text{Bu}_4\text{NPF}_6$  solutions (Table 1). In the anodic scan, only the oxidation of the metal complex<sup>[24, 25]</sup> could be observed for **F-Re** and **F-Ru**. In the cathodic region, **F-Re** and **F-Ru** show two reversible one-electron reduction processes followed by a dielectronic peak. As shown by the comparison with model compounds **F**, **Re**, and **Ru**, the two

Table 1. Electrochemical properties of **F–Re**, **F–Ru**, **Re**, **Ru**, and **F** determined by CV on a glassy carbon working electrode in  $\text{CH}_2\text{Cl}_2 + 0.1\text{M } n\text{Bu}_4\text{NPF}_6$  solutions at room temperature.<sup>[a]</sup>

Compound	Reduction			Oxidation
	$E_1$	$E_2$	$E_3$	$E_1$
<b>F</b> <sup>[b]</sup>	–1.03 (59)	–1.41 (80)	–1.84 (110)	
<b>Re</b>	–1.88 (80)			+0.92 <sup>[c,d]</sup>
<b>F–Re</b>	–0.99 (70)	–1.37 (80)	–1.83 (140) <sup>[e]</sup>	+0.96 <sup>[e]</sup>
<b>Ru</b>	–1.76 (80)			+0.92 (90)
<b>F–Ru</b>	–1.02 (80)	–1.40 (80)	–1.81 (100) <sup>[e]</sup>	+0.91 (70)

[a] Values for  $(E_{\text{pa}} + E_{\text{pc}})/2$  in V vs. Fc<sup>+/0</sup> and  $\Delta E_{\text{pc}}$  in mV (in parentheses) at a scan rate of 0.1 V s<sup>–1</sup>. [b] From ref. [19]. [c] Irreversible process,  $E_{\text{pa}}$  value reported. [d] Reversible for  $V > 1$  V s<sup>–1</sup>. [e] Dielectronic process.

first waves correspond to  $\text{C}_{60}$ -centered reductions and the third peak to the simultaneous reduction of the metal complex<sup>[24, 25]</sup> and the fullerene. Interestingly, in the case of **F–Re**, the two first fullerene-centered reduction potentials are shifted to more positive values by about 40 mV with respect to the corresponding fullerene model compound **F**. On the other hand, the metal-centered oxidation potential is found to be more positive in **F–Re** when compared to **Re**. The latter observations could be a consequence of small electronic interactions between the rhenium(i) complex and the methanofullerene unit in **F–Re**, suggesting that this compound may adopt a folded conformation in which the two moieties are close to each other. This is in agreement with previous reports in which derivatives with a metal center and a fullerene unit, forced to be spatially close, behave similarly (more facile fullerene reduction, harder metal-centered oxidation).<sup>[18]</sup> This effect is not observed in the case of **F–Ru**, the oxidation and reduction potentials being substantially unchanged when compared to those of the corresponding model compounds **F** and **Ru**. In this case, the charged ruthenium(ii) complex and the carbon sphere are likely to be far from each other. In other words, **F–Ru** must adopt an extended conformation preventing sizeable electronic interactions among the two moieties in the dyad.

**Photophysical properties and photoinduced processes:** The electronic absorption spectra of the reference compounds **F**, **Re**, and **Ru** in  $\text{CH}_2\text{Cl}_2$  (Figure 1) are in agreement with previous reports. The  $\text{C}_{60}$  fullerene **F** exhibits intense absorp-

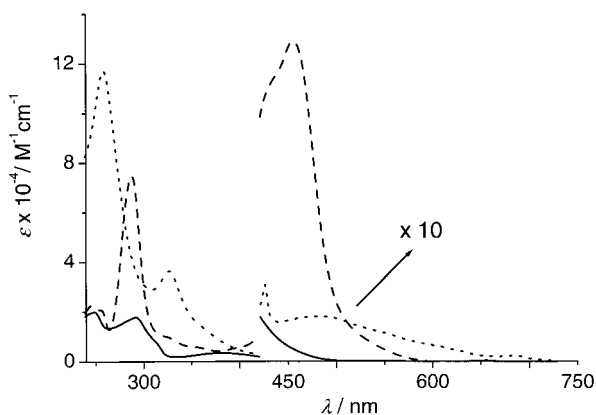


Figure 1. Absorption spectrum of **F** (.....), **Re** (—), and **Ru** (---) in  $\text{CH}_2\text{Cl}_2$ ; in the region above 420 nm the spectra are multiplied by a factor of 10.

tion bands in the UV, whereas weaker features are observed in the Vis region, with the diagnostic methanofullerene bands at 426 ( $\epsilon = 3000\text{M}^{-1}\text{cm}^{-1}$ ) and 687 nm ( $\epsilon = 200\text{M}^{-1}\text{cm}^{-1}$ ).<sup>[21, 26]</sup> In the UV side, **Re** and **Ru** display ligand-centered (LC) bpy-type bands with a spectral peak at around 290 nm. The spectral features in the Vis spectral region are attributed to <sup>1</sup>MLCT transitions, which lie higher in energy for **Re** ( $\lambda_{\text{max}} = 382$  nm) than for **Ru** ( $\lambda_{\text{max}} = 456$  nm), as expected.<sup>[27, 28]</sup>

The absorption spectra of **F–Re** and **F–Ru** in  $\text{CH}_2\text{Cl}_2$  are depicted in Figure 2 and match the profiles obtained by summing the spectra of the component units within an experimental uncertainty of  $\pm 15\%$ . For **F–Re**, the absorption features of the  $\text{C}_{60}$  unit largely dominate the entire spectral profile, unlike **F–Ru**. Importantly, in the case of **F–Ru** an

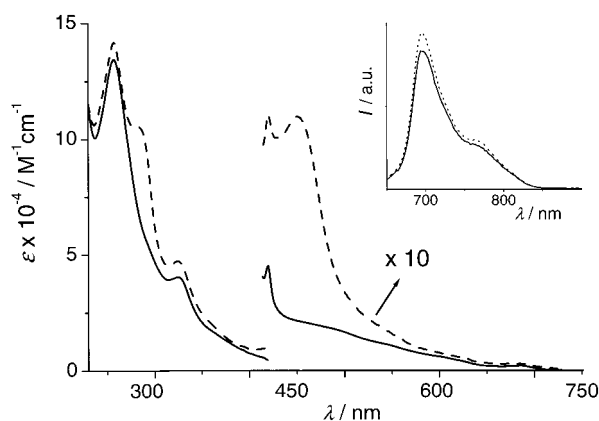


Figure 2. Absorption spectrum of **F–Re** (—) and **F–Ru** (---) in  $\text{CH}_2\text{Cl}_2$ ; in the region above 420 nm the spectra are multiplied by a factor of 10. Inset: fluorescence spectra of isoabsorbing solutions (O.D. = 0.200) of **F** (.....) and **F–Re** (—);  $\lambda_{\text{exc}} = 550$  nm, where only the  $\text{C}_{60}$  moiety absorbs in **F–Re**. Identical fluorescence relative intensities are obtained by comparing the spectra of **F** and **F–Ru** upon excitation at 625 nm.

almost selective excitation of the metal-complexed moiety ( $\geq 85\%$ ) is possible at 456 nm, corresponding to the maximum of the MLCT absorption band. At  $\lambda > 600$  nm the  $\text{C}_{60}$  moiety can be excited exclusively. In contrast, selective excitation of the  $\text{Re}^{\text{I}}$  moiety is not possible in **F–Re** and the highest extent of excitation of such a unit is achieved at 292 and 380 nm, that is 35 and 30%, respectively. Conversely, selective excitation of the  $\text{C}_{60}$  moiety is possible at any wavelength above 490 nm.

Table 2 summarizes the emission properties and excited state lifetimes of the reference compounds **F**, **Ru**, **Re**, and of the dyads **F–Re** and **F–Ru**, both in  $\text{CH}_2\text{Cl}_2$  at 298 K and in a  $\text{CH}_2\text{Cl}_2/\text{MeOH}$  (1:1, v/v) 77 K glass.

**F** exhibits the typical short-lived methanofullerene fluorescence band peaked at 698 nm (Figure 2),<sup>[21, 26]</sup> that is also observable at 77 K ( $\lambda_{\text{max}} = 706$  nm). The latter result allows the location of the lowest singlet fullerene excited state at 1.78 eV. Attempts to detect phosphorescence with time-gated techniques were unsuccessful, as were attempts using glasses containing heavy atom solvents such as ethyl iodide.<sup>[29]</sup> We therefore take the energy value of the lowest fullerene triplet excited state to be 1.50 eV, as earlier estimated for methanofullerenes by theoretical calculations.<sup>[21]</sup>

Table 2. Luminescence properties in CH<sub>2</sub>Cl<sub>2</sub> at 298 K and in CH<sub>2</sub>Cl<sub>2</sub>/MeOH (1:1 v/v) at 77 K.

	298 K, C <sub>60</sub> Fluo			298 K, MLCT Band			77 K, C <sub>60</sub> Fluo		77 K, MLCT Band	
	$\lambda_{\max}^{[a]}$ [nm]	$\Phi_{\text{em}}^{[b]}$ [ $\times 10^4$ ]	$\tau^{[c]}$ [ns]	$\lambda_{\max}^{[a]}$ [nm]	$\Phi_{\text{em}}^{[b]}$ [ $\times 10^2$ ]	$\tau^{[c]}$ [ns]	$\lambda_{\max}^{[a]}$ [nm]	$\tau^{[c]}$ [ns]	$\lambda_{\max}^{[a]}$ [nm]	$\tau^{[c]}$ [ns]
<b>F</b>	696 (698)	4.1	1.0				706 (706)	1.6		
<b>Re</b>				585 (625)	1.2 (1.5)	75 (102)			518 (530)	5300
<b>F–Re</b>	696 <sup>[d]</sup> (698)	3.6	0.8	582 <sup>[e]</sup> (622)	$\approx 0.02$	3.8	698 <sup>[d]</sup> (700)	1.7	508 <sup>[e]</sup> (524)	3.7
<b>Ru</b>				605 (616)	4.3 (8.5)	448 (1009)			578 (580)	7300
<b>F–Ru</b>	698 <sup>[f]</sup> (702)	3.7	1.0	605 <sup>[g]</sup> (616)	$\approx 0.07$	4.4	694 <sup>[f]</sup> (696)	1.7	578 <sup>[g]</sup> (580)	6800

[a] Emission maxima from uncorrected and, in parentheses, corrected spectra. [b] Emission quantum yields in air-equilibrated and, in parentheses, air-free solutions. [c] Excited state lifetimes in air-equilibrated and, in parentheses, air-free solutions,  $\lambda_{\text{exc}} = 337$  nm. [d]  $\lambda_{\text{exc}} = 550$  nm. [e]  $\lambda_{\text{exc}} = 380$  nm. [f]  $\lambda_{\text{exc}} = 625$  nm. [g]  $\lambda_{\text{exc}} = 456$  nm.

**Re** and **Ru** exhibit the typically intense and long-lived MLCT luminescence bands at room temperature and 77 K (Table 2, Figure 3).

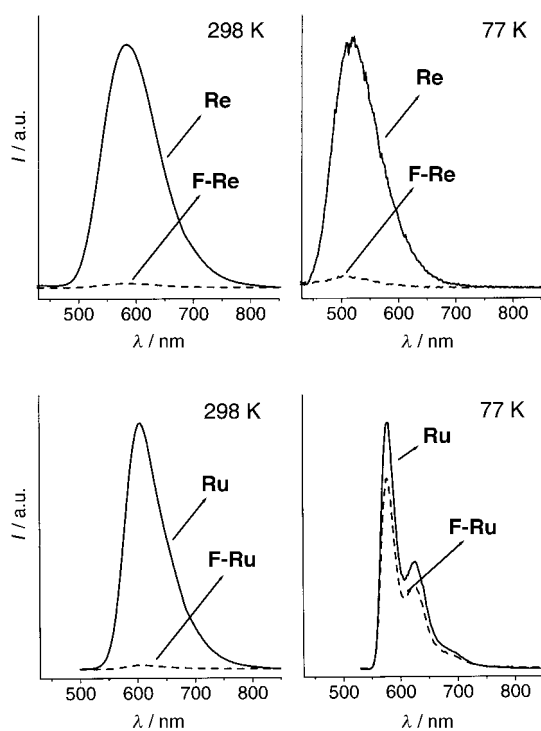


Figure 3. Top: <sup>3</sup>MLCT Luminescence spectra of **Re** and **F–Re** at 298 K (CH<sub>2</sub>Cl<sub>2</sub> solution) and 77 K (CH<sub>2</sub>Cl<sub>2</sub>/MeOH 1:1 v/v);  $\lambda_{\text{exc}} = 292$  nm, isoabsorbing solutions (O.D. = 0.350). Bottom: <sup>3</sup>MLCT Luminescence spectra of **Ru** and **F–Ru** at 298 K (CH<sub>2</sub>Cl<sub>2</sub> solution) and 77 K (CH<sub>2</sub>Cl<sub>2</sub>/MeOH 1:1 v/v);  $\lambda_{\text{exc}} = 456$  nm, isoabsorbing solutions (O.D. = 0.200).

It is worth pointing out that at 298 K the emission band of **Re** is broader than that of **Ru** and the corresponding maximum in **Re** is slightly red-shifted relative to **Ru**. Conversely, at 77 K, the **Re** band is substantially blue-shifted, if compared to that of **Ru**. This trend can be explained by considering that **Re** is a neutral complex which, upon MLCT excitation, brings about a larger solvent reorganization than the doubly charged **Ru** complex.<sup>[28]</sup> Consequently, in a rigid matrix, because of lack of solvent repolarization, the MLCT

excited states of **Re** are more destabilized than those of **Ru**. The **Re** complex is also characterized by a larger Stokes shift (SS) relative to **Ru**, that is 6600 versus 2100 cm<sup>-1</sup>, as can be obtained from Equation (1).<sup>[28]</sup>

$$SS = E_{\text{abs}} - E_{\text{em}} - E_{\text{S-T}} \quad (1)$$

In Equation (1)  $E_{\text{abs}}$  and  $E_{\text{em}}$  are, respectively, the maxima of the absorption (<sup>1</sup>MLCT) and emission (<sup>3</sup>MLCT) bands at 298 K, and  $E_{\text{S-T}}$  is the energy difference between the lowest <sup>1</sup>MLCT and <sup>3</sup>MLCT excited states, estimated to be about 3600 cm<sup>-1</sup> for electronically similar Os<sup>II</sup> complexes.<sup>[28]</sup> This difference in SS values is reflected in the wider emission band profile exhibited by **Re**.

The most important consequence of these peculiarities in **Re** and **Ru** photophysics is the difference in energy of the lowest MLCT excited state, which is estimated to be 2.37 and 2.14 eV, respectively, from the 77 K emission band maxima. This apparently slight variation is the origin of a significantly different trend in photoinduced processes for the dyads **F–Re** and **F–Ru**, as will be discussed below.

Upon excitation at 550 (**F–Re**) and 625 nm (**F–Ru**), where only the C<sub>60</sub> chromophore absorbs, the typical methanofullerene fluorescence band is substantially unaffected for both dyads if compared to that of the reference compound **F** (Table 2, Figure 2). This indicates that intercomponent photoinduced processes do not occur when the C<sub>60</sub> chromophore is excited.

On the contrary, when excitation is addressed to the metal complex moiety, intercomponent excited-state events are evidenced for both dyads. The emission spectrum of **F–Re** following light excitation at 292 nm (35% of light on the **Re** moiety, see above) show that: 1) the strong and long-lived MLCT luminescence of the **Re** unit is substantially quenched (Table 2, Figure 3); 2) the C<sub>60</sub> fluorescence yield is reduced by about 35% relative to reference compound **F** (Figure 4). Similar results are obtained for **F–Ru** (Table 2, Figure 3, and Figure 5) but in this case the excitation can be more selective (see above). Importantly, for both dyads, when excitation is addressed where both moieties absorb, the measured quantum yield of C<sub>60</sub> fluorescence reflects the amount of light directly exciting the fullerene moiety (Figure 4 and Figure 5).

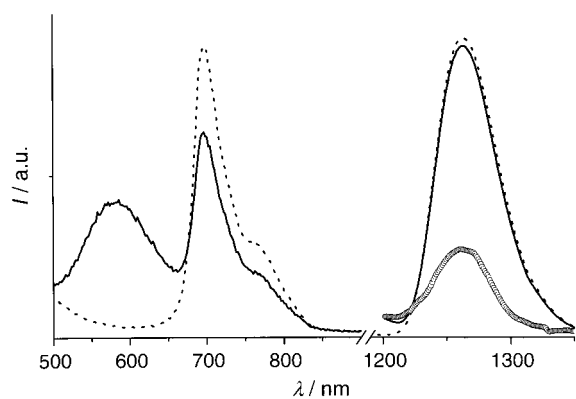


Figure 4. Fluorescence spectra of isoabsorbing solutions (O. D. = 0.450) of **F** (····) and **F-Re** (—).  $\lambda_{\text{exc}} = 292$  nm, where 30% of the incident light is addressed to the metal-complexed moiety **F-Re**. In the IR region are reported the sensitized singlet oxygen luminescence bands of isoabsorbing solutions (O.D. = 0.200) of **F** (····), **Re** (○), and **F-Re** (—),  $\lambda_{\text{exc}} = 380$  nm.

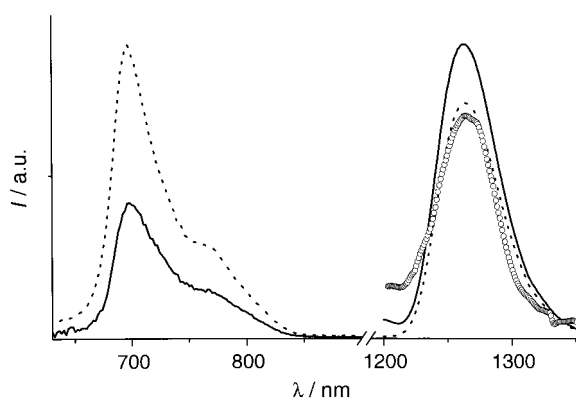


Figure 5. Fluorescence spectra of isoabsorbing solutions (O.D. = 0.170) of **F** (····) and **F-Ru** (—);  $\lambda_{\text{exc}} = 510$  nm, where light is equally partitioned between the two chromophores. From the spectrum of **F-Ru** the background of the residual (quenched)  $^3\text{MLCT}$  emission has been subtracted. In the IR region are reported the sensitized singlet oxygen luminescence bands of isoabsorbing solutions (O.D. = 0.200) of **F** (····), **Ru** (○), and **F-Ru** (—),  $\lambda_{\text{exc}} = 456$  nm.

This suggests that 1) photoinduced processes are not triggered by excitation of the  $\text{C}_{60}$  moiety; 2) the  $^3\text{MLCT}$  excited state of the metal-complexed moiety does not sensitize the lowest fullerene singlet excited state.

As far as the quenching of the  $^3\text{MLCT}$  excited states is concerned, time-resolved luminescence spectroscopy allows the calculation of the rate constants of the quenching processes ( $k_q$ ) by means of Equation (2) ( $\tau$  and  $\tau_0$  are the lifetimes of the quenched and unquenched  $^3\text{MLCT}$  excited states), which turn out to be practically identical, that is  $2.5 \times 10^8 \text{ s}^{-1}$  (**F-Re**) and  $2.3 \times 10^8 \text{ s}^{-1}$  (**F-Ru**).

$$k_q = 1/\tau - 1/\tau_0 \quad (2)$$

On the basis of the energy of the lowest excited states of the various moieties, as determined by emission spectroscopy, an energy level diagram for the two dyads can be drawn (Figure 6). Importantly, for both dyads, the electrochemical results allow the location of a charge-separated state (CS) corresponding to the reduction of the  $\text{C}_{60}$  moiety and the oxidation of the metal-complexed unit [ $\text{F}^-\text{-M}^+$ ].<sup>[30]</sup> Owing to

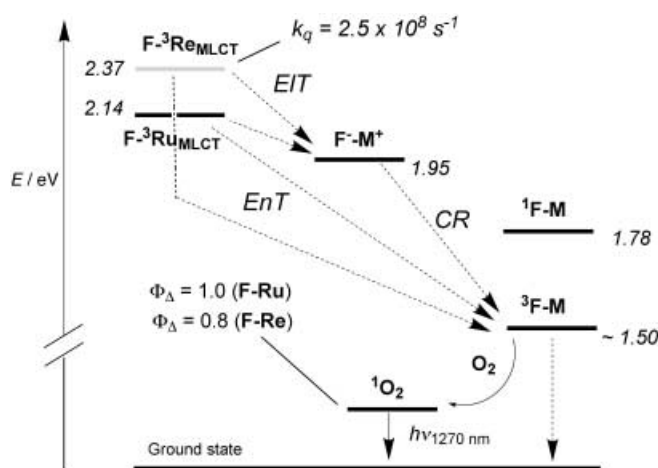


Figure 6. Energy level diagram for **F-Ru** and **F-Re**. The localized excited-state energies are estimated from the 77 K emission band maxima, while the position of the CS state is obtained from the electrochemical data. The  $\text{F}^-\text{-M}^+$  CS level and fullerene localized excited states are indicated with a single notation since they are identical for both dyads.

its energy position ( $\approx 1.95$  eV in both cases), such a CS state might play an active role in the cascade of photoinduced processes following  $^3\text{MLCT}$  excitation.

From the diagram of Figure 6 it is evident that, in principle, two different processes can account for the observed  $^3\text{MLCT}$  luminescence quenching in the two dyads: 1) electron-transfer leading to the [ $\text{F}^-\text{-M}^+$ ] (namely  $\text{F}^-\text{-Re}^{2+}$  or  $\text{F}^-\text{-Ru}^{3+}$ ) CS state or 2) energy transfer to the lowest fullerene triplet state. Energy transfer to the lowest fullerene singlet excited states is ruled out because luminescence data do not show any fullerene fluorescence sensitization (see above).

To investigate in detail the excited state dynamics within the **F-Re** and **F-Ru** dyads, transient absorption studies would be useful but are hampered by the unfavourable light partition on the metal-complexed moiety at the wavelengths of our Nd:YAG laser flash-photolysis instrumentation. For **F-Re** the situation is extremely unfavourable because the **Re** moiety does not absorb at 532 nm and, at 266 and 355 nm, nearly 90% of light is absorbed by the  $\text{C}_{60}$  unit. Under these circumstances any experimental effort to investigate photoinduced processes arising from the **Re**-complexed fragment can hardly give reliable results. The most favourable case is that of **F-Ru** where, at 532 nm, the **Ru** moiety absorbs about 30% of the incident light. The transient absorption spectrum of **F-Ru** at  $\lambda_{\text{exc}} = 532$  nm is shown in Figure 7. It displays a maximum at 690 nm and is practically identical to that of the reference compound **F** under the same conditions. We can therefore safely attribute it to the triplet-triplet transient absorption spectrum of the fullerene unit.<sup>[21, 26]</sup>

Importantly, the rise of the transient absorption signal is identical for **F-Ru** and **F**, indicating that the  $^3\text{F-Ru}$  is formed at a faster rate than our instrumental resolution (20 ns). The fullerene triplet lifetimes of **F**, **F-Re**, and **F-Ru** in air-equilibrated and argon-saturated solution are reported in Table 3; they show sizeable differences, which are commented on below.

Because of the difficulties of studying in detail the photoinduced excited-state dynamics within the two dyads by

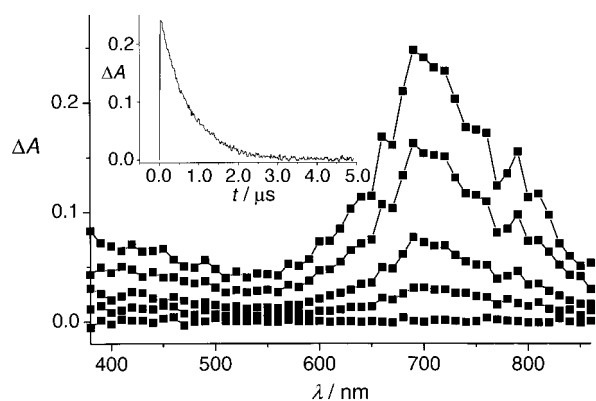


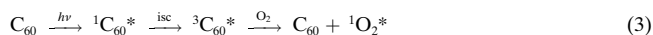
Figure 7. Transient absorption ( $\Delta A$ ) spectrum of **F-Ru** at 298 K in  $\text{CH}_2\text{Cl}_2$  air-equilibrated solution upon laser excitation at 532 nm (energy = 5 mJ per pulse). The spectra were recorded at delays of 100, 400, 900, 1500, and 4000 ns following excitation. The inset shows the time profile of  $\Delta A$  (690 nm) from which the spectral kinetic data were obtained; the fitting is monoexponential and gives a lifetime of 755 ns.

Table 3. Fullerene triplet lifetimes in  $\text{CH}_2\text{Cl}_2$  aerated and deaerated solutions as determined by transient absorption spectroscopy.

	Aerated [ns]	Deaerated [ns]
<b>F</b>	714	24 600
<b>F-Re</b>	776	14 900
<b>F-Ru</b>	755	18 000

means of transient absorption spectroscopy, a different approach was attempted aimed at determining the yield of formation of the lowest available excited level, that is the fullerene triplet (Figure 6). This yield can give valuable clues about excited state intercomponent processes involving upper-lying levels.

It is known that light excitation of pristine  $\text{C}_{60}$  populates the lowest singlet excited state ( $^1\text{C}_{60}^*$ ) that is then converted to the lowest triplet state ( $^3\text{C}_{60}^*$ ) with nearly unitary yield ( $\Phi_{\text{T}} = 1$ ) by intersystem crossing (isc).<sup>[31, 32]</sup> In air-equilibrated solution  $^3\text{C}_{60}^*$  is then quenched by dioxygen, that is sensitized to its  $^1\Delta(\text{O}_2)$  excited state, which deactivates back to the ground state giving rise to emission in the IR spectral region ( $\lambda_{\text{max}} = 1268 \text{ nm}$ ).<sup>[33]</sup> The whole sensitization process can be schematized as in Equation (3), where  $^1\text{O}_2^*$  stands for  $\text{O}_2(^1\Delta_{\text{g}})$ , commonly named “singlet oxygen”.



The yield of sensitization of  $^1\text{O}_2^*$  is termed  $\Phi_{\Delta}$  and is unity for pristine  $\text{C}_{60}$ .<sup>[32]</sup> The  $\Phi_{\text{T}}$  values of substituted fullerenes are lower than 1<sup>[34, 35]</sup> and are reported to be 0.8 for methanofullerenes.<sup>[21, 34]</sup> Importantly, the values of  $\Phi_{\Delta}$  and  $\Phi_{\text{T}}$  are found to be identical for  $\text{C}_{60}$  and its closed-cage<sup>[26]</sup> or open-cage<sup>[36]</sup> derivatives as well as for higher fullerenes such as  $\text{C}_{70}$ <sup>[37]</sup> and  $\text{C}_{76}$ .<sup>[38]</sup> Therefore, the measure of  $\Phi_{\Delta}$  can be taken as an indirect evaluation of  $\Phi_{\text{T}}$  for all fullerenes.<sup>[39]</sup>

We first determined the  $\Phi_{\Delta}$  of the reference fullerene compound **F** (0.8) using as reference  $\text{C}_{60}$  ( $\Phi_{\Delta} = 1$ ). The  $^1\text{O}_2$  emission bands of solutions containing **F-Re** ( $\lambda_{\text{exc}} = 380 \text{ nm}$ ) and **F-Ru** ( $\lambda_{\text{exc}} = 456 \text{ nm}$ ), and their corresponding model compounds, are reported in Figures 4 and 5.

In the case of **F-Ru**, the results are straightforward. Despite the fact that its components are characterized by  $\Phi_{\Delta}$  values of 0.8 (**F**) and 0.7 (**Ru**), for **F-Ru** a higher amount of singlet oxygen is formed corresponding to  $\Phi_{\Delta} = 1.0$ . This means that the  $^3\text{F-Ru}$  state is formed with unitary yield ( $\Phi_{\text{T}} = 1.0$ ) and confirms that the fullerene lowest singlet state (less efficient in forming the triplet state,  $\Phi_{\text{T}} = 0.8$  for **F**) is not involved in photoinduced processes following  $^3\text{MLCT}$  excitation.

The situation is different for **F-Re** for which  $\Phi_{\Delta} = 0.8$  is found. This value is higher than that expected admitting no fullerene triplet sensitization from the  $^3\text{MLCT}$  state, that is 0.6, taking into account the interchromophoric light partition at 380 nm and the low  $\Phi_{\Delta}$  of **Re** (0.25, see Figure 4). Therefore, we have to conclude that the fullerene triplet is sensitized in **F-Re**, though to a lesser extent (80%) than **F-Ru** (100%).

We can argue whether in our dyads the fullerene triplet population is obtained 1) by direct triplet-triplet (T-T) EnT from the  $^3\text{MLCT}$  of the metal-complexed unit, or 2) through an EIT leading to  $\text{F}^-\text{M}^+$  followed by charge recombination to the fullerene triplet (Figure 6). Earlier studies suggest that T-T (Dexter-type) EnT processes display strong similarities with electron-transfer processes and can be treated by a similar formalism.<sup>[40, 41]</sup> In the case of dyads made of a  $\text{Re}^{\text{I}}$  complex and an aromatic subunit the rate constant of T-T EnT as a function of reaction thermodynamics obeys a Marcus-type behavior, where the maximum rate is obtained for  $\Delta G^{\circ} \approx -0.3 - 0.4 \text{ eV}$ .<sup>[42]</sup> In our case  $\Delta G^{\circ} = -0.87$  (**F-Re**) and  $-0.64 \text{ eV}$  (**F-Ru**), so it is reasonable to assume that the T-T EnT process is positioned in the inverted region, whereas the lower exoergonicity of the competing CS processes ( $\Delta G_{\text{CS}}^{\circ}$  in the range 0.2–0.4 eV) is optimal to locate the EIT process in the proximity of the maximum of the Marcus parabola as has been found, for instance, in  $\text{Zn}^{\text{II}}$ -porphyrins/ $\text{C}_{60}$  molecular dyads.<sup>[43]</sup> The same thermodynamic arguments apply to the CR process which is likely to be faster in giving the  $\text{C}_{60}$  triplet ( $\Delta G^{\circ} \approx -0.55 \text{ eV}$ ) rather than the ground state ( $\Delta G_{\text{CR}}^{\circ} \approx -1.95 \text{ eV}$ ). Therefore, on the basis of the above considerations, we would tend to ascribe the quenching of the MLCT excited states to electron transfer rather than to direct triplet-triplet energy transfer.

To find evidence supporting the EIT mechanism, we recorded 77 K luminescence spectra for **F-Re** and **F-Ru** to check if there is any difference relative to the room-temperature behavior. It is in fact known that the energy of a charge-separated state is expected to increase in a rigid matrix, where the effective solvent reorganization energy increases dramatically because the solvent molecules cannot reorientate to stabilize the newly formed ions.<sup>[44]</sup> Hence, when the EIT process is slightly exoergonic at room temperature, it may become endoergonic (blocked) at 77 K. Consequently, for multicomponent arrays where the occurrence of photoinduced processes is signaled by luminescence quenching in solution, the lack of such quenching in a rigid matrix is taken as evidence to support the EIT mechanism in the fluid medium. Very interestingly, the  $^3\text{MLCT}$  emission of the metal-complexed moiety is recovered for **F-Ru** (Figure 3)<sup>[45]</sup> and a lifetime of 6.8  $\mu\text{s}$  is measured, which is identical within experimental uncertainties (see Experimental Section) to

that of **Ru** (7.3  $\mu$ s). This suggests that triplet–triplet energy transfer, though thermodynamically allowed, is extremely inefficient at 77 K and is not able to compete with intrinsic deactivation of the **Ru** moiety, which gives rise to its typical  $^3$ MLCT emission. Importantly, since the rates of energy-transfer processes are known to be scarcely affected by temperature,<sup>[46]</sup> we can also argue that at 298 K, EnT can hardly compete with EIT deactivation. Finally, the fact that at 77 K the  $^3$ MLCT emission quenching is not observed for **F–Ru** strongly supports the electron-transfer mechanism at 298 K for the  $^3$ MLCT excited state (see above).

For **F–Re**, recovery of the  $^3$ MLCT luminescence is not observed at 77 K (Figure 3), and a quenched lifetime of 3.7 ns is determined (to be compared to 5.3  $\mu$ s for **Re**), corresponding to a quenching rate constant of  $2.7 \times 10^8 \text{ s}^{-1}$  [Eq. (1)]. We believe that this can be explained considering the higher energy of the  $^3$ MLCT level, if compared to **F–Ru**. A 0.42 eV difference between  $^3$ MLCT and the CS state (Figure 6) is likely to be too large to make the electron-transfer reaction endoergonic at 77 K, as it happens for **F–Ru** ( $\Delta G^\circ = -0.19 \text{ eV}$ ). Accordingly, the  $^3$ MLCT excited state of **F–Re** is quenched by electron transfer even in a 77 K rigid matrix, also because the EnT mechanism is likely to be as inefficient as in the case of **F–Ru**, given the similarity of the involved thermodynamic parameters (Figure 6).

As for the low  $\Phi_\Delta$  value found for **F–Re**, it is noteworthy that the **Re** chromophore is neutral, unlike that of **Ru** which bears a double positive charge. This could give different conformations of the two dyads in solution, also considering the flexible nature of the linker. The hydrophobic fullerene fragment could be in tighter vicinity with the metal-complexed counterpart in the case of **F–Re**, and this could shield the  $C_{60}$  unit from the interaction with  $O_2$  molecules (a well documented “physical” effect for carbon spheres),<sup>[34, 47]</sup> thus leading to a lower  $\Phi_\Delta$  value. This shielding would imply that, in this case, the assumption  $\Phi_\Delta = \Phi_T$  cannot be applied and, despite the fact that the fullerene triplet sensitization is quantitative, its usual “probe” ( $^1O_2$  luminescence) cannot be profitably employed due to structural reasons. To support this hypothesis we note that the excited state lifetimes of the fullerene singlet (Table 2) and triplet (Table 3, air-free solution) is the lowest for **F–Re**, when compared to **F–Ru** and **F**. This suggests faster intersystem crossing processes, possibly favored by close vicinity with the heavy-atom complexed moiety. On the other hand, the fact that the air-equilibrated triplet lifetime is the longest for **F–Re**, seems to give further support to the hypothesis of a substantial protective action exerted by the  $Re^I$  chromophore on the  $C_{60}$  carbon sphere, even able to counterbalance the heavy-atom effect under these conditions. Finally, this is in good agreement with the electrochemical data suggesting spatial proximity for the two chromophores in **F–Re** but not in **F–Ru**.

## Conclusion

Two dyads, **F–Re** and **F–Ru**, in which a methanofullerene moiety is coupled with a metal complex unit such as

[ $Re(bpy)CO_3Br$ ] or [ $Ru(bpy)_3$ ]<sup>2+</sup> have been prepared, and their electrochemical and photophysical properties have been investigated. We have showed that, in  $CH_2Cl_2$  at 298 K, light excitation of the lowest  $^3$ MLCT excited states of the  $Re^I$ - and  $Ru^{II}$ -complexed moieties is followed by electron transfer to the  $C_{60}$  counterpart, followed by quantitative charge recombination to the lowest fullerene-centered triplet-excited state ( $^3C_{60}$ ), as determined by singlet oxygen sensitization experiments. The direct triplet–triplet energy-transfer quenching route ( $^3$ MLCT  $\rightarrow$   $^3C_{60}$ ) is uncompetitive with electron transfer. As far as the  $Ru^{II}$ -complexed dyad is concerned, the photophysical results reported here show some differences if compared to related dyads made of  $Ru^{II}$  coordination compounds and fulleropyrrolidines in  $CH_2Cl_2$  solution, as reported by Guldi et al. In particular, in a series of papers those authors show that quenching of the  $^3$ MLCT excited states are due to 1) electron transfer followed by repopulation of the  $^3$ MLCT level,<sup>[19]</sup> 2) electron transfer followed by charge recombination to the ground state,<sup>[17]</sup> or 3) direct T–T energy transfer to the  $C_{60}$  triplet.<sup>[16]</sup>

The different trends observed can be explained by some differences for chromophores, for example, methanofullerenes (this work) versus fulleropyrrolidines (Guldi et al.) or for linkers, for example, flexible<sup>[17]</sup> versus rigid.<sup>[16, 19]</sup> In particular, for the above case (3)<sup>[16]</sup> the MLCT level of the  $Ru^{II}$  chromophore is very low-lying (1.75 eV, since a strong  $\pi$ -acceptor chelating ligand is used: dpq = 2,3-bipyridin-2-yl-quinoline), thus making the triplet–triplet EnT route much more thermodynamically favoured ( $\Delta G^\circ \approx -0.25 \text{ eV}$ ) than in our case.

Interesting differences are found in the behavior of the two dyads of the present work. In particular: 1) EIT is blocked in a rigid matrix for **F–Ru** but not for **F–Re**, thanks to the different energy location of the  $^3$ MLCT levels in the two cases; 2) the quantum yield of singlet oxygen sensitization is lower for **F–Re**, and this is explained by means of structural arguments, corroborated by electrochemical and photophysical experimental findings. This latter effect is being investigated in our laboratories, by studying complexes with a larger number of fullerene units.

It has been shown earlier that low-lying triplets such as those of fullerene,<sup>[48, 49]</sup> free-base porphyrin,<sup>[50]</sup> or carotene<sup>[51]</sup> can offer efficient charge-recombination routes to upper-lying charge-separated states in several fullerene-containing multicomponent arrays. In the present work we show that this is also the case for dyads containing  $Re^I$  and  $Ru^{II}$  metal-complexed units where, although photoinduced electron transfer is effective, the final product of photoinduced processes is the low-lying fullerene lowest triplet ( $^3C_{60}^*$ ).

We believe that this outcome must be carefully taken into account in the design of fullerene multicomponent systems containing  $Re^I$  and  $Ru^{II}$  metal complexes. In fact, in a solvent of intermediate polarity like  $CH_2Cl_2$ , we find that the energy difference between the CS and  $^3C_{60}$  states is rather high ( $\approx 0.45 \text{ eV}$ ). This suggests that, even in a more polar solvent like benzonitrile,<sup>[50]</sup> it is hard to depress the CS state energy so as to eliminate such an energy gap. Accordingly, for this kind of dyad, fast deactivation to  $^3C_{60}$  constitutes a formidable obstacle for obtaining high yields of long-lived and highly

exoergonic CS states that can be exploited for practical applications.

In turn, our present findings suggest that in order to build up fullerene dyads with metal complexes displaying low-lying MLCT levels, the choice should be oriented to more reducing MLCT excited states. In this way it would be possible to lower the CS level below 1.5 eV and make it the final destination of photoinduced processes, before charge recombination. In this regard, Cu<sup>I</sup>-phenanthrolines, owing to their electrochemical and excited state properties,<sup>[13]</sup> seem to be more promising candidates with respect to Re<sup>I</sup> or Ru<sup>II</sup>-bipyridines.<sup>[21]</sup> We are currently working along this line.

## Experimental Section

**General:** Reagents and solvents were purchased as reagent grade and used without further purification. THF was distilled over sodium benzophenone ketyl. Compounds 4-bromobutyl tetrahydropyran-2-yl ether,<sup>[23]</sup> **F**<sup>[22]</sup> and **4**<sup>[22]</sup> were prepared as previously reported. All reactions were performed in standard glassware in an inert Ar atmosphere. Evaporation and concentration were performed at water aspirator pressure, and drying was in vacuo at 10<sup>-2</sup> Torr. Column chromatography: silica gel 60 (230–400 mesh, 0.040–0.063 mm) was purchased from E. Merck. Thin-layer chromatography (TLC) was performed on glass sheets coated with silica gel 60F<sub>254</sub> purchased from E. Merck, visualization by UV light. IR spectra (cm<sup>-1</sup>) were measured on an ATI Mattson Genesis Series FTIR instrument. NMR spectra were recorded on a Bruker AC200 with solvent peaks as reference. Mass spectra (MS) were obtained on an electrospray (ES) triple quadrupole mass spectrometer Quattro II with a mass-to-charge (*m/z*) ratio range extended to 8000 (Micromass, Altrincham, UK). Sample solutions were introduced into the mass spectrometer source with a syringe pump (Harvard type 551111: Harvard Apparatus Inc., South Natick, MA, USA) with a flow rate of 6 μL min<sup>-1</sup>. Calibration was performed using protonated horse myoglobin. Scanning was performed in the MCA (Multi Channel Analyzer) mode, and several scans were summed to obtain the final spectrum. Elemental analyses were performed by the analytical service at the Institut Charles Sadron, Strasbourg.

**Compound 2:** A 2 M solution of lithium diisopropylamide (LDA) in THF (5.4 mL) was added slowly to a solution of 4,4'-dimethyl-2,2'-bipyridine (2.00 g, 10.85 mmol) in anhydrous THF (60 mL) at 0 °C under Ar. After 1 h, a solution of 4-bromobutyl tetrahydropyran-2-yl ether (3.10 g, 13.02 mmol) in THF (25 mL) was added dropwise. The resulting mixture was stirred for 2 h at 0 °C, then 15 h at room temperature. The solution was then poured into ice water (150 mL). The mixture was extracted with Et<sub>2</sub>O (3 × 100 mL) and the combined organic layers were dried (MgSO<sub>4</sub>), filtered and evaporated. Column chromatography (SiO<sub>2</sub>, CH<sub>2</sub>Cl<sub>2</sub>) yielded **2** (2.36 g, 64%) as a pale yellow oil. <sup>1</sup>H NMR (CDCl<sub>3</sub>, 200 MHz): δ = 1.24–1.81 (m, 12H), 2.44 (s, 3H), 2.71 (t, *J* = 6 Hz, 2H), 3.41 (m, 2H), 3.76 (m, 2H), 4.58 (t, *J* = 6 Hz, 1H), 7.13 (m, 2H), 8.24 (brs, 2H), 8.56 (m, 2H).

**Compound 3:** A solution of **2** (830 mg, 2.44 mmol) and *p*-TsOH (682 mg, 4.87 mmol) in EtOH (200 mL) was refluxed for 24 h. The solvent was then evaporated. Column chromatography (Al<sub>2</sub>O<sub>3</sub>, CH<sub>2</sub>Cl<sub>2</sub> containing 0.5% MeOH) yielded **3** (360 mg, 58%) as a colorless oil. <sup>1</sup>H NMR (CDCl<sub>3</sub>, 200 MHz): δ = 1.38–1.90 (m, 6H); 2.43 (s, 3H); 2.71 (t, *J* = 6 Hz, 2H); 3.64 (t, *J* = 6 Hz, 2H); 7.13 (m, 2H); 8.22 (s, 2H); 8.55 (m, 2H); <sup>13</sup>C NMR (CDCl<sub>3</sub>, 50 MHz): δ = 21.17, 25.39, 30.08, 32.47, 35.38, 62.63, 121.30, 122.09, 123.95, 124.66, 148.28, 148.81, 148.94, 152.61.

**Compound 1:** DCC (168 mg, 0.814 mmol) was added to a stirred solution of **4** (1.00 g, 0.814 mmol), **3** (167 mg, 0.651 mmol), DMAP (16 mg, 0.130 mmol), and BiOH (catalytic amount) in CH<sub>2</sub>Cl<sub>2</sub> (50 mL) at 0 °C. After 1 h, the mixture was allowed to slowly warm to room temperature (within 1 h), then stirred for 12 h, filtered and evaporated. Column chromatography (SiO<sub>2</sub>, CH<sub>2</sub>Cl<sub>2</sub> containing 2% MeOH) yielded **1** (750 mg, 78%) as a dark red glassy product. <sup>1</sup>H NMR (CDCl<sub>3</sub>, 200 MHz): δ = 0.89 (t, *J* = 6 Hz, 6H), 1.45 (m, 26H), 1.77 (m, 4H), 2.50 (s, 3H), 2.75 (t, *J* = 7 Hz, 2H), 3.90 (t, *J* = 6 Hz, 4H), 4.24 (t, *J* = 7 Hz, 2H),

4.95 (s, 2H), 5.46 (s, 2H), 6.40 (t, *J* = 2 Hz, 1H), 6.60 (d, *J* = 2 Hz, 2H), 7.20 (m, 2H), 8.36 (brs, 2H), 8.55 (m, 2H); <sup>13</sup>C NMR (CDCl<sub>3</sub>, 50 MHz): δ = 14.09, 21.15, 22.62, 25.42, 26.06, 28.28, 29.22, 29.34, 29.88, 31.77, 35.21, 51.26, 62.54, 65.57, 68.05, 69.05, 71.12, 101.57, 107.19, 121.20, 122.03, 123.81, 124.62, 125.22, 128.15, 128.96, 136.49, 138.36, 139.71, 140.83, 141.69, 141.82, 142.08, 142.81, 142.90, 143.71, 143.76, 144.40, 144.54, 144.79, 144.85, 145.08, 148.11, 148.81, 148.94, 152.19, 155.80, 156.00, 160.38, 162.91, 166.40; IR (CH<sub>2</sub>Cl<sub>2</sub>):  $\tilde{\nu}$  = 1748 cm<sup>-1</sup> (C=O); elemental analysis calcd (%) for C<sub>104</sub>H<sub>60</sub>N<sub>2</sub>O<sub>8</sub>: C 85.23, H 4.13, N 1.91; found: C 85.21, H 4.27, N 1.95.

**Compound F–Ru:** A mixture of *cis*-dichloro-bis(2,2'-bipyridine)ruthenium(II) dihydrate (16.5 mg, 0.034 mmol) and silver tetrafluoroborate (16.6 mg, 0.085 mmol) in acetone (10 mL) was refluxed for 2 h. After the mixture had been cooled and filtered, the solvent was removed and the mixture taken up in DMF (10 mL). Compound **1** (50 mg, 0.0341 mmol) was then added. The resulting mixture was refluxed for 3 h. After the mixture had cooled, the crude product was precipitated as its PF<sub>6</sub> salt by addition of a methanolic solution of NH<sub>4</sub>PF<sub>6</sub> (NH<sub>4</sub>PF<sub>6</sub> (2 g) in MeOH (50 mL)) followed by water. The brown solid was filtered, washed with water, MeOH, and Et<sub>2</sub>O. Column chromatography (SiO<sub>2</sub>, CH<sub>2</sub>Cl<sub>2</sub> containing 10% MeOH) followed by recrystallization from CH<sub>2</sub>Cl<sub>2</sub>/hexane yielded **F–Ru** (30 mg, 40%) as a dark red powder. <sup>1</sup>H NMR (CDCl<sub>3</sub>, 200 MHz): δ = 0.86 (t, *J* = 6 Hz, 6H), 1.28 (m, 26H), 1.72 (m, 4H), 2.51 (s, 3H), 2.81 (m, 2H), 3.88 (t, *J* = 6 Hz, 4H), 4.21 (m, 2H), 4.95 (s, 2H), 5.46 (s, 2H), 6.39 (t, *J* = 2 Hz, 1H), 6.58 (d, *J* = 2 Hz, 2H), 7.26 (m, 2H), 7.43 (m, 6H), 7.70 (m, 4H), 7.95 (m, 4H), 8.25 (m, 6H); <sup>13</sup>C NMR (CDCl<sub>3</sub>, 50 MHz): δ = 14.12, 21.20, 22.64, 25.51, 26.09, 28.14, 29.24, 29.37, 31.77, 35.12, 35.22, 51.36, 62.63, 65.52, 68.09, 69.15, 71.18, 101.62, 107.32, 121.20, 122.04, 123.83, 124.18, 124.65, 128.02, 129.05, 136.55, 137.83, 138.30, 139.76, 140.80, 141.69, 141.85, 142.10, 142.85, 142.94, 143.75, 144.43, 144.54, 144.63, 144.84, 145.12, 148.88, 149.00, 150.14, 150.62, 151.20, 154.21, 155.97, 156.27, 156.54, 156.62, 156.69, 160.40, 162.97, 166.54; MS (ES): 2024.1 [M – PF<sub>6</sub>]<sup>+</sup>; 939.3 [M – 2PF<sub>6</sub>]<sup>2+</sup>; elemental analysis calcd for C<sub>124</sub>H<sub>76</sub>N<sub>6</sub>O<sub>8</sub>RuP<sub>2</sub>F<sub>12</sub>: C 68.67, H 3.53, N 3.87; found: C 68.69, H 3.83, N 3.60.

**Compound Ru:** A mixture of *cis*-dichloro-bis(2,2'-bipyridine)ruthenium(II) dihydrate (100 mg, 0.23 mmol) and silver tetrafluoroborate (112 mg, 0.575 mmol) in acetone (10 mL) was refluxed for 2 h. After the mixture had been cooled and filtered, the solvent was removed and the mixture taken up in DMF (10 mL). 4,4'-dimethyl-2,2'-bipyridine (42.4 mg, 0.23 mmol) was then added. The resulting mixture was refluxed for 3 h. After the mixture had cooled, the crude product was precipitated as its PF<sub>6</sub> salt by addition of a methanolic solution of NH<sub>4</sub>PF<sub>6</sub> (NH<sub>4</sub>PF<sub>6</sub> (2 g) in MeOH (50 mL)) followed by water. The solid was filtered, washed with water, MeOH and Et<sub>2</sub>O. Recrystallization from CH<sub>3</sub>CN/toluene yielded **Ru** (168 mg, 82%) as an orange solid. <sup>1</sup>H NMR (CD<sub>2</sub>Cl<sub>2</sub>, 200 MHz): δ = 2.50 (s, 6H), 7.24 (m, 2H), 7.46 (m, 6H), 7.71 (m, 4H), 8.04 (m, 6H), 8.25 (brs, 2H), 8.42 (m, 2H); elemental analysis calcd for C<sub>32</sub>H<sub>28</sub>N<sub>6</sub>RuP<sub>2</sub>F<sub>12</sub> · H<sub>2</sub>O: C 42.44, H 3.34, N 9.28; found: C 42.18, H 3.66, N 9.25.

**Compound F–Re:** A solution of **1** (100 mg, 0.068 mmol) and [Re(CO)<sub>3</sub>Br] (27.7 mg, 0.068 mmol) in toluene (100 mL) was refluxed for 2 h. The reaction mixture was cooled to room temperature and evaporated to dryness. The residue was dissolved in a minimum amount of CH<sub>2</sub>Cl<sub>2</sub> and slowly added to a cold solution of pentane. The resulting red precipitate was filtered and dried under vacuum to yield **F–Re** (80 mg, 64%) as a red powder. <sup>1</sup>H NMR (CDCl<sub>3</sub>, 200 MHz): δ = 0.88 (t, *J* = 6 Hz, 6H), 1.30 (m, 26H), 1.77 (m, 4H), 2.57 (s, 3H), 2.81 (t, *J* = 6 Hz, 2H), 3.89 (t, *J* = 6 Hz, 4H), 4.27 (t, *J* = 6 Hz, 2H), 4.96 (s, 2H), 5.47 (s, 2H), 6.41 (t, *J* = 2 Hz, 1H), 6.60 (d, *J* = 2 Hz, 2H), 7.31 (m, 2H), 7.95 (s, 1H), 8.00 (s, 1H), 8.88 (d, *J* = 6 Hz, 1H), 8.90 (d, *J* = 6 Hz, 1H); <sup>13</sup>C NMR (CDCl<sub>3</sub>, 50 MHz): δ = 14.08, 21.59, 22.60, 25.37, 26.03, 28.17, 29.18, 29.31, 29.50, 31.73, 35.33, 51.98, 62.57, 65.24, 68.06, 69.04, 71.09, 101.49, 107.19, 123.05, 123.98, 126.91, 127.78, 136.46, 138.31, 139.68, 140.77, 141.60, 141.79, 142.04, 142.82, 142.90, 143.70, 144.32, 144.37, 144.50, 144.76, 145.04, 145.13, 151.14, 152.45, 152.66, 155.10, 155.20, 155.38, 160.37, 162.66, 162.95, 166.43, 189.05, 196.88; IR (CH<sub>2</sub>Cl<sub>2</sub>):  $\tilde{\nu}$  = 2021, 1918, 1896 (C=O), 1750 cm<sup>-1</sup> (C=O); elemental analysis calcd for C<sub>107</sub>H<sub>60</sub>N<sub>2</sub>O<sub>11</sub>ReBr: C 70.78, H 3.33, N 1.54; found: C 71.02, H 3.48, N 1.31.

**Compound Re:** A solution of 4,4'-dimethyl-2,2'-bipyridine (45.3 mg, 0.025 mmol) and [Re(CO)<sub>3</sub>Br] (100 mg, 0.025 mmol) in toluene (10 mL) was refluxed for 2 h. The reaction mixture was cooled to room temperature and evaporated to dryness. The residue was dissolved in a minimum amount of CH<sub>2</sub>Cl<sub>2</sub> and slowly added to a cold solution of pentane. The resulting yellow precipitate was filtered and dried under vacuum to yield



**Re** (101 mg, 76 %) as a yellow powder.  $^1\text{H NMR}$  ( $\text{CD}_2\text{Cl}_2$ , 200 MHz):  $\delta = 2.58$  (s, 6H), 7.36 (dd,  $J = 1$  and 6 Hz, 2H), 8.03 (d,  $J = 1$  Hz, 2H), 8.85 (d,  $J = 6$  Hz, 2H); IR ( $\text{CH}_2\text{Cl}_2$ ): 2020, 1916, 1895  $\text{cm}^{-1}$  (C=O); elemental analysis calcd for  $\text{C}_{15}\text{H}_{12}\text{N}_2\text{O}_3\text{ReBr}$ : C 33.71, H 2.26, N 5.24; found: C 33.81, H 2.42, N 5.18.

**Electrochemistry:** The electrochemical studies were carried out in  $\text{CH}_2\text{Cl}_2$  (Fluka, spectroscopic grade used without further purification) containing 0.1 M  $\text{Bu}_4\text{NPF}_6$  (Merck, electrochemical grade) as supporting electrolyte. A standard three-electrode cell was connected to a computerized electrochemical device Autolab (Eco Chemie B.V. Utrecht, Holland). The working electrode was a glassy carbon disk (3 mm in diameter), the auxiliary electrode a platinum wire, and the reference electrode an aqueous Ag/AgCl reference electrode. All potentials are given versus Fc/Fc<sup>+</sup> used as internal standard.

**Photophysical measurements:** The spectroscopic investigations were carried out in  $\text{CH}_2\text{Cl}_2$  (Carlo Erba, spectrofluorimetric grade). The samples were placed in fluorimetric 1-cm-path cuvettes and, when necessary, purged of oxygen by bubbling Ar for 5 min. Absorption spectra were recorded with a Perkin-Elmer  $\lambda 40$  spectrophotometer. Uncorrected emission spectra were obtained with a Spex Fluorolog II spectrofluorimeter (continuous 150 W Xe lamp), equipped with a Hamamatsu R-928 photomultiplier tube. The corrected spectra were obtained using a calibration curve determined with a previously described procedure.<sup>[52]</sup> Fluorescence quantum yields obtained from spectra on an energy scale ( $\text{cm}^{-1}$ ) were measured with the method described by Demas and Crosby<sup>[53]</sup> using as standards air-equilibrated solutions of  $[\text{Ru}(\text{bpy})_3]^{2+}$  in water ( $\Phi_{\text{em}} = 0.028$ )<sup>[54]</sup> or  $[\text{Os}(\text{phen})_3]^{2+}$  in acetonitrile ( $\Phi_{\text{em}} = 0.005$ ).<sup>[55]</sup> Attempts to obtain delayed phosphorescence spectra were performed with the above mentioned Spex Fluorolog II spectrometer equipped with a pulsed Xe lamp (1934D Phosphorimeter). To record the 77 K luminescence spectra, the samples were put in glass tubes (2 mm diameter) and inserted in a special quartz dewar, filled up with liquid nitrogen. When necessary, spectra of the glass matrix were recorded and then subtracted as a background signal, in order to eliminate the contribution from light scattering.

The steady-state IR luminescence spectra were obtained with a constructed-in-house apparatus available at the Chemistry Department of the University of Bologna (Italy) and described in detail earlier.<sup>[52]</sup> A continuous 450 W Xe lamp was used as a light source in order to be able to excite at 380 and 456 nm (see Discussion). The determination of the yields of singlet oxygen sensitization, according to Darmanyan and Foote,<sup>[56]</sup> was obtained by monitoring the steady-state singlet oxygen luminescence intensity at 1268 nm and taking  $\text{C}_{60}$  in  $\text{CH}_2\text{Cl}_2$  as the relative standard ( $\Phi_{\Delta} = 1.0$ ).<sup>[21]</sup> Solutions with the same optical density and solvent ( $\text{CH}_2\text{Cl}_2$ ) were used, making corrections due to these factors unnecessary.<sup>[56]</sup>

Emission lifetimes on the nanosecond time scale were determined with an IBH single-photon-counting spectrometer equipped with a thyatron-gated nitrogen lamp working in the range 2–40 KHz ( $\lambda_{\text{exc}} = 337$  nm, 0.5 ns time resolution); the detector was a red-sensitive (185–850 nm) Hamamatsu R-3237-01 photomultiplier.

The transient absorption spectra and fullerene triplet lifetimes were obtained by using the second harmonic (532 nm) of a Nd:YAG laser (JK Lasers) with 2 ns pulse and 1–2 mJ of energy per pulse. The details on the flash-photolysis system are reported elsewhere.<sup>[57]</sup>

Experimental uncertainties are estimated to be  $\pm 8\%$  for lifetime determinations,  $\pm 20\%$  for emission quantum yields,  $\pm 5\%$  for relative emission intensities in the NIR,  $\pm 1$  nm and  $\pm 5$  nm for absorption and emission peaks respectively.

## Acknowledgements

This work was supported by the CNR, the CNRS and the French Ministry of Research (ACI Jeunes Chercheurs). We thank the Laboratoire d'Electrochimie et de Chimie Physique du Corps Solide (UMR 7512, Strasbourg) for the CV measurements, L. Oswald for technical help, and Prof. A. Juris (Department of Chemistry, University of Bologna) for allowing the use of the IR spectrofluorimeter. G.A. thanks Italian MIUR (Progetto 5 %) and D.F. the Région Alsace for their research fellowships. We also thank Prof. M. Gross for helpful discussions.

- [1] D. Gust, T. A. Moore, A. L. Moore, *Acc. Chem. Res.* **2001**, *34*, 40–48.
- [2] D. M. Guldi, *Chem. Commun.* **2000**, 321–327.
- [3] H. Imahori, Y. Sakata, *Eur. J. Org. Chem.* **1999**, 2445–2457.
- [4] N. Martin, L. Sanchez, B. Illescas, I. Perez, *Chem. Rev.* **1998**, *98*, 2527–2547.
- [5] F. Diederich, C. Thilgen, *Science* **1996**, *271*, 317–323.
- [6] H. Imahori, D. M. Guldi, K. Tamaki, Y. Yoshida, C. P. Luo, Y. Sakata, S. Fukuzumi, *J. Am. Chem. Soc.* **2001**, *123*, 6617–6628.
- [7] D. Kuciauskas, P. A. Liddell, S. Lin, T. E. Johnson, S. J. Weghorn, J. S. Lindsey, A. L. Moore, T. A. Moore, D. Gust, *J. Am. Chem. Soc.* **1999**, *121*, 8604–8614.
- [8] N. Armaroli, C. Boudon, D. Felder, J. P. Gisselbrecht, M. Gross, G. Marconi, J. F. Nicoud, J. F. Nierengarten, V. Vicinelli, *Angew. Chem.* **1999**, *111*, 3895–3899; *Angew. Chem. Int. Ed.* **1999**, *38*, 3730–3733.
- [9] L. C. Sun, L. Hammarstrom, B. Akermark, S. Styring, *Chem. Soc. Rev.* **2001**, *30*, 36–49.
- [10] C. J. Brabec, N. S. Sariciftci, J. C. Hummelen, *Adv. Funct. Mater.* **2001**, *1*, 15–26.
- [11] J. F. Eckert, J. F. Nicoud, J. F. Nierengarten, S. G. Liu, L. Echegoyen, F. Barigelletti, N. Armaroli, L. Ouali, V. Krasnikov, G. Hadziioannou, *J. Am. Chem. Soc.* **2000**, *122*, 7467–7479.
- [12] V. Balzani, A. Juris, *Coord. Chem. Rev.* **2001**, *211*, 97–115.
- [13] N. Armaroli, *Chem. Soc. Rev.* **2001**, *30*, 113–124.
- [14] V. W. W. Yam, *Chem. Commun.* **2001**, 789–796.
- [15] L. De Cola, P. Belser, *Coord. Chem. Rev.* **1998**, *177*, 301–346.
- [16] D. M. Guldi, M. Maggini, E. Menna, G. Scorrano, P. Ceroni, M. Marccaccio, F. Paolucci, S. Roffia, *Chem. Eur. J.* **2001**, *7*, 1597–1605.
- [17] A. Polese, S. Mondini, A. Bianco, C. Toniolo, G. Scorrano, D. M. Guldi, M. Maggini, *J. Am. Chem. Soc.* **1999**, *121*, 3446–3452.
- [18] D. Armspach, E. C. Constable, F. Diederich, C. E. Housecroft, J. F. Nierengarten, *Chem. Eur. J.* **1998**, *4*, 723–733.
- [19] M. Maggini, D. M. Guldi, S. Mondini, G. Scorrano, F. Paolucci, P. Ceroni, S. Roffia, *Chem. Eur. J.* **1998**, *4*, 1992–2000.
- [20] N. S. Sariciftci, F. Wudl, A. J. Heeger, M. Maggini, G. Scorrano, M. Prato, J. Bourassa, P. C. Ford, *Chem. Phys. Lett.* **1995**, *247*, 510–514.
- [21] N. Armaroli, F. Diederich, C. O. Dietrich-Buchecker, L. Flamigni, G. Marconi, J. F. Nierengarten, J. P. Sauvage, *Chem. Eur. J.* **1998**, *4*, 406–416.
- [22] D. Felder, H. Nierengarten, J. P. Gisselbrecht, C. Boudon, E. Leize, J. F. Nicoud, M. Gross, A. Van Dorsselaer, J. F. Nierengarten, *New J. Chem.* **2000**, *24*, 687–695.
- [23] P. C. Wälchli, C. H. Eugster, *Helv. Chim. Acta* **1978**, *61*, 885–898.
- [24] T. M. Miller, K. J. Ahmed, M. S. Wrighton, *Inorg. Chem.* **1989**, *28*, 2347–2355.
- [25] C. F. Shu, M. S. Wrighton, *Inorg. Chem.* **1988**, *27*, 4326–4329.
- [26] R. V. Bensasson, E. Bienvenue, C. Fabre, J. M. Janot, E. J. Land, S. Leach, V. Leboulaire, A. Rassat, S. Roux, P. Seta, *Chem. Eur. J.* **1998**, *4*, 270–278.
- [27] P. R. Ashton, V. Balzani, A. Credi, O. Kocian, D. Pasini, L. Prodi, N. Spencer, J. F. Stoddart, M. S. Tolley, M. Venturi, A. J. P. White, D. J. Williams, *Chem. Eur. J.* **1998**, *4*, 590–607.
- [28] D. A. Bardwell, F. Barigelletti, R. L. Cleary, L. Flamigni, M. Guardigli, J. C. Jeffery, M. D. Ward, *Inorg. Chem.* **1995**, *34*, 2438–2446.
- [29] F. Prat, C. Marti, S. Nonell, X. J. Zhang, C. S. Foote, R. G. Moreno, J. L. Bourdelande, J. Font, *Phys. Chem. Chem. Phys.* **2001**, *3*, 1638–1643.
- [30] V. Balzani, F. Scandola, *Supramolecular Photochemistry*, Ellis Horwood, Chichester, **1991**, pp. 44–45.
- [31] J. W. Arbogast, A. P. Darmanyan, C. S. Foote, Y. Rubin, F. N. Diederich, M. M. Alvarez, S. J. Anz, R. L. Whetten, *J. Phys. Chem.* **1991**, *95*, 11–12.
- [32] R. R. Hung, J. J. Grabowski, *J. Phys. Chem.* **1991**, *95*, 6073–6075.
- [33] F. Wilkinson, W. P. Helman, A. B. Ross, *J. Phys. Chem. Ref. Data* **1995**, *24*, 663–1021.
- [34] T. Hamano, K. Okuda, T. Mashino, M. Hirobe, K. Arakane, A. Ryu, S. Mashiko, T. Nagano, *Chem. Commun.* **1997**, 21–22.
- [35] C. Luo, M. Fujitsuka, A. Watanabe, O. Ito, L. Gan, Y. Huang, C. H. Huang, *J. Chem. Soc. Faraday Trans.* **1998**, *94*, 527–532.
- [36] R. Stackow, G. Schick, T. Jarrosson, Y. Rubin, C. S. Foote, *J. Phys. Chem. B* **2000**, *104*, 7914–7918.

- [37] R. V. Bensasson, M. Schwell, M. Fanti, N. K. Wachter, J. O. Lopez, J.-M. Janot, P. R. Birkett, E. J. Land, S. Leach, P. Seta, R. Taylor, F. Zerbetto, *Chem. Phys. Chem.* **2001**, 109–114.
- [38] R. V. Bensasson, E. Bienvenue, J. M. Janot, E. J. Land, S. Leach, P. Seta, *Chem. Phys. Lett.* **1998**, 283, 221–226.
- [39] K. Kordatos, T. Da Ros, M. Prato, S. Leach, E. J. Land, R. V. Bensasson, *Chem. Phys. Lett.* **2001**, 334, 221–228.
- [40] V. Balzani, F. Bolletta, F. Scandola, *J. Am. Chem. Soc.* **1980**, 102, 2152–2163.
- [41] V. Balzani, F. Scandola, *J. Chem. Ed.* **1983**, 60, 814.
- [42] D. B. Macqueen, J. R. Eyler, K. S. Schanze, *J. Am. Chem. Soc.* **1992**, 114, 1897–1898.
- [43] H. Imahori, N. V. Tkachenko, V. Vehmanen, K. Tamaki, H. Lemmetinen, Y. Sakata, S. Fukuzumi, *J. Phys. Chem. A* **2001**, 105, 1750–1756.
- [44] P. Y. Chen, T. J. Meyer, *Inorg. Chem.* **1996**, 35, 5520–5524.
- [45] Apparently, the recovery of intensity is not complete if compared to **Ru** under the same conditions (see Figure 3). However, taking into account several factors, it can be safely assessed that the recovery is complete within the experimental errors. In particular, one has to consider: 1) the high experimental uncertainties in detecting luminescence spectra of rigid matrices; 2) the (minimal) fraction of light absorbed by the fullerene moiety in **F-Ru**; 3) possible differences in the optical density of the two samples at 77 K, despite identical values at 298 K.
- [46] L. Hammarström, F. Barigelletti, L. Flamigni, N. Armaroli, A. Sour, J. P. Collin, J. P. Sauvage, *J. Am. Chem. Soc.* **1996**, 118, 11972–11973.
- [47] F. Prat, R. Stackow, R. Bernstein, W. Y. Qian, Y. Rubin, C. S. Foote, *J. Phys. Chem. A* **1999**, 103, 7230–7235.
- [48] E. Peeters, P. A. van Hal, J. Knol, C. J. Brabec, N. S. Sariciftci, J. C. Hummelen, R. A. J. Janssen, *J. Phys. Chem. B* **2000**, 104, 10174–10190.
- [49] D. M. Guldi, S. Gonzalez, N. Martin, A. Anton, J. Garin, J. Orduna, *J. Org. Chem.* **2000**, 65, 1978–1983.
- [50] C. Luo, D. M. Guldi, H. Imahori, K. Tamaki, K. Sakata, *J. Am. Chem. Soc.* **2000**, 122, 6535–6551.
- [51] J. L. Bahr, D. Kuciauskas, P. A. Liddell, A. L. Moore, T. A. Moore, D. Gust, *Photochem. Photobiol.* **2000**, 72, 598–611.
- [52] N. Armaroli, G. Marconi, L. Echegoyen, J. P. Bourgeois, F. Diederich, *Chem. Eur. J.* **2000**, 6, 1629–1645.
- [53] J. N. Demas, G. A. Crosby, *J. Phys. Chem.* **1971**, 75, 991.
- [54] K. Nakamaru, *Bull. Chem. Soc. Jpn.* **1982**, 55, 2697–2705.
- [55] E. M. Kober, J. V. Caspar, R. S. Lumpkin, T. J. Meyer, *J. Phys. Chem.* **1986**, 90, 3722–3734.
- [56] A. P. Darmanyan, C. S. Foote, *J. Phys. Chem.* **1993**, 97, 5032–5035.
- [57] L. Flamigni, *J. Phys. Chem.* **1992**, 96, 3331–3337.

Received: November 2, 2001 [F3649]